Science Advances
AAAS

advances.sciencemag.org/cgi/content/full/5/9/eaat9461/DC1

Supplementary Materials for

Paramagnon drag in high thermoelectric figure of merit Li-doped MnTe

Y. Zheng, T. Lu, Md M. H. Polash, M. Rasoulianboroujeni, N. Liu, M. E. Manley, Y. Deng, P. J. Sun, X. L. Chen, R. P. Hermann*, D. Vashaee*, J. P. Heremans*, H. Zhao*

*Corresponding author. Email: heremans.1@osu.edu (J.P.H.); hzhao@iphy.ac.cn (H.Z.); dvashae@ncsu.edu (D.V.); hermannrp@ornl.gov (R.P.H.)

Published 13 September 2019, *Sci. Adv.* **5**, eaat9461 (2019)
DOI: 10.1126/sciadv.aat9461

This PDF file includes:

SUPPLEMENTARY MATERIALS

Density function theory (DFT) calculations:
The first-principles calculations were performed with the CASTEP program code using the plane-wave pseudopotential method. The generalized gradient approximation (GGA) was adopted in the form of the Perdew−Burke−Ernzerhof for the exchange-correlation potentials. Spin-polarized and LDA+U calculations were made to account for the MnTe system correctly. The ultrasoft pseudopotential was used with a plane-wave energy cutoff of 410 eV. The first Brillouin zone was sampled with a grid spacing of 0.037 $Å^{-1}$. The self-consistent field was set as 5×10^{-7} eV/atom. Both lattice parameters and atomic positions were optimized with the Broyden, Fletcher, Goldfarb, and Shannon (BFGS) method until an energy change of less than 5×10^{-6} eV/atom, residual force less than 0.01 eV/Å, and max stress less than 0.02 GPa were achieved. A 2×2×2 supercell was used to study the electronic structure of undoped and Li-doped MnTe.

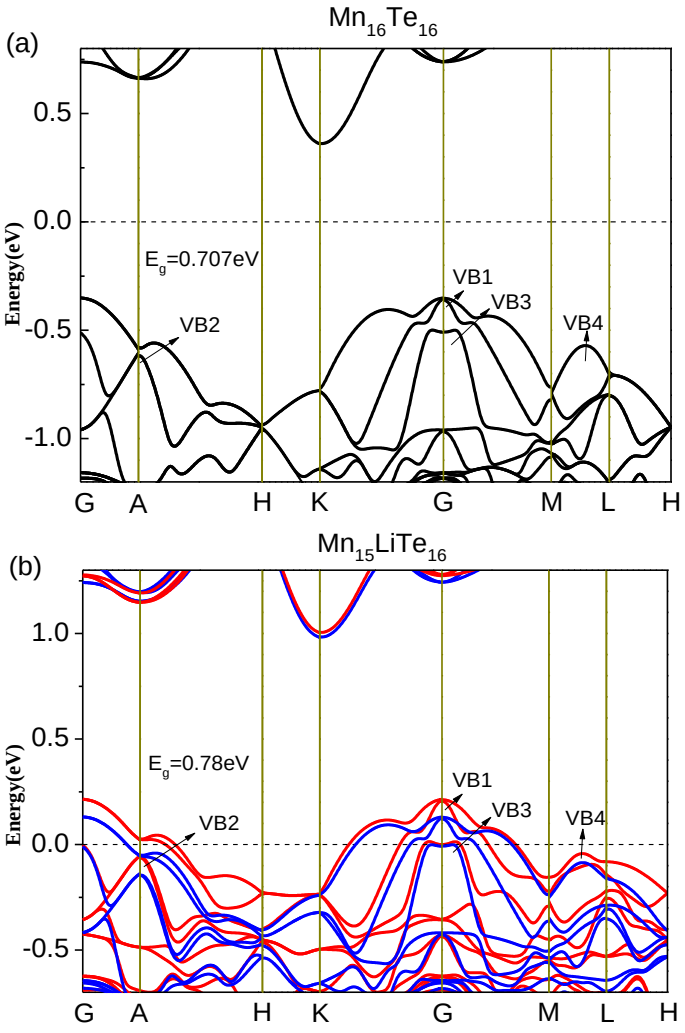

Fig. S1. Band structures of paramagnetic and antiferromagnetic hexagonal MnTe. Band structure, (a) in the paramagnetic state (nominally undoped sample) (b) in the antiferromagnetic state (sample nominally doped with x=0.062 Li).

Non-intentionally doped MnTe

The high vapor pressure of both Mn and Te, the tendency of Mn to oxidize, and the complex defect chemistry of chalcogenide semiconductors do not allow for the control of the unintentional doping level of binary MnTe. As a result, the free charge carrier concentration of non-intentionally-doped binary MnTe varies in the mid-10^{17}cm^{-3} range, and sample-to-sample reproducibility of the transport data is not sufficiently satisfactory to report data in the main text. Still, both magnon drag and paramagnon drag are observed in binary MnTe, as is seen in fig. S2. At $T > 500$ K, both the resistivity and the thermopower decrease, presumably as a result of the appearance of thermally excited minority electrons.

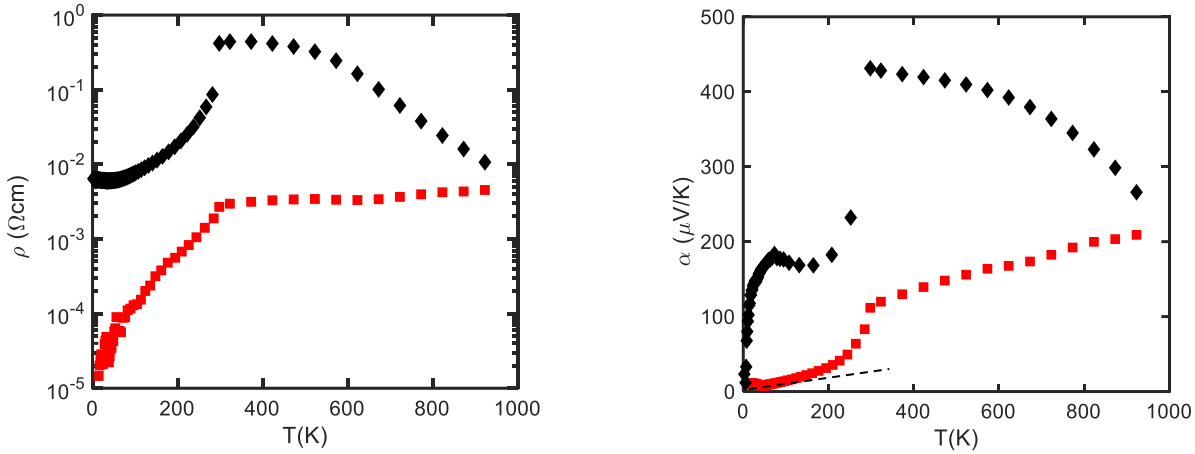

Fig. S2. Comparison of the resistivity (left frame) and thermopower (right frame) of non-intentionally doped binary MnTe (black diamonds) and MnTe doped with 3% Li (red squares).

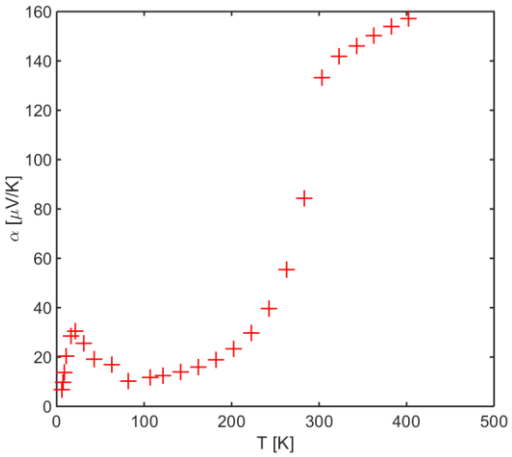

Fig. S3. Phonon drag in Li-MnTe. Below 50K, the samples with 0.3% and 1% Li doping show an additional phonon drag peak. This is visible in fig. S2 as a small excess above the dashed line. The data on the sample with 1% Li doping are more clear and are shown in fig. S3.